

## Direct Observation of Many-Electron Magnetoconductivity in a Nondegenerate 2D Electron Liquid

M. J. Lea, P. Fozooni, and P. J. Richardson

*Department of Physics, Royal Holloway, University of London, Egham, Surrey TW20 0EX, England*

A. Blackburn

*Department of Electronics and Computer Science, University of Southampton, Southampton SO17 1BJ, England*  
(Received 25 April 1994)

The magnetoconductivity  $\sigma(B)$  of two-dimensional electrons on liquid helium was measured above 1 K, using high-precision Corbino electrodes. In low magnetic fields  $B$ ,  $\sigma(0)/\sigma(B) = 1 + (\mu B)^2$  as in the Drude model, where  $\mu$  is the zero-field mobility due to scattering by  $^4\text{He}$  vapor atoms, even for  $\mu B \gg 1$ . At higher fields  $\sigma(0)/\sigma(B)$  becomes density dependent due to many-electron effects, in excellent agreement with the theory of Dykman. Only at the highest fields, or the lowest densities, does  $\sigma(B)$  approach the theoretical single-particle magnetoconductivity.

PACS numbers: 73.20.Dx, 67.90.+z, 73.50.Jt

Electrons above the surface of superfluid helium form a nearly ideal two-dimensional electron system (2DES). At the electron densities,  $n < 2 \times 10^{13} \text{ m}^{-2}$ , which are stable on bulk liquid, the electrons are nondegenerate and are perhaps the best example of a classical 2D conducting system [1]. The electrons are held in a vertical potential well produced by the repulsion of the helium surface and an applied vertical electric pressing field. At low temperatures  $T$  they are in the quantum ground state for vertical motion but are free to move horizontally. The electrons are scattered by  $^4\text{He}$  vapor atoms above 1 K and by surface ripplon modes on the helium at lower temperatures where the zero-field mobility  $\mu$  can be as high as  $10^3 \text{ m}^2/\text{V s}$ . The matrix elements for the scattering are well known [2] and give good agreement with the experimental values for  $\mu(T)$  [3]. Vapor atoms act as almost ideal point-scattering centers with quasielastic scattering (due to the large mass ratio). The application of a vertical magnetic field  $B$  to this system is particularly interesting for  $\mu B > 1$ , the region of classically strong magnetic fields. In the single-electron approximation the energy spectrum becomes a series of discrete quantized Landau levels, energy separation  $\hbar\omega_c$ , where  $\omega_c = eB/m$  is the cyclotron frequency. The extreme quantum limit,  $\hbar\omega_c/kT = 1.344B/T > 1$ , in which only the lowest Landau level is occupied, is easily reached. However, the Coulomb interaction between electrons gives a fluctuating many-electron electric field which changes the discrete Landau levels into a continuous spectrum and strongly influences the magnetotransport in the quantum region. This was first recognized by Dykman who gave theoretical expressions for ripplon [4,5] and vapor atom scattering [6].

The Drude model for the magnetoconductivity  $\sigma_{xx}(B)$  of a classical 2DES assumes classical cyclotron orbits [radius  $R_c = (2mkT)^{1/2}/eB$ ] and a field-independent scattering rate and gives

$$\frac{\sigma_0}{\sigma_{xx}(B)} = \frac{1}{\sigma^*(B)} = 1 + (\mu B)^2, \quad (1)$$

where  $\sigma_0 = \sigma_{xx}(0) = ne\mu$  is the zero-field conductivity. It is equivalent to the Einstein relation  $\sigma_{xx} = ne^2L^2/kT\tau$  where  $L$  is the diffusion length ( $\propto$  orbit radius in high fields) and  $1/\tau$  is the scattering rate. The formation of Landau levels changes the energy density of states and hence the scattering rate becomes field dependent. The quantum cyclotron radius must also be used in quantizing magnetic fields. Both these effects are included in the orbit migration theory in the self-consistent Born approximation (SCBA) for magnetoconductivity  $\sigma_s$  [7] for a nondegenerate 2DES [8,9] with  $\sigma_{xx} \ll \sigma_{xy}$ . An extension of this theory [10] to all values of  $\sigma_{xx}/\sigma_{xy}$  was used here. For  $\mu B \gg 1$  this gives  $1/\sigma_s^*(B) \propto (\mu B)^{3/2}$  for  $\hbar\omega_c/kT \ll 1$ , and  $1/\sigma_s^*(B) \propto B^{1/2}\mu^{3/2}$  for  $\hbar\omega_c/kT \gg 1$ . But the SCBA is a noninteracting independent particle theory and, for all but the lowest electron densities, the Dykman many-electron effect [4–6] changes the energies of neighboring cyclotron orbits and reduces the diffusion rate and  $\sigma_{xx}(B)$ . These many-electron effects “restore” the Drude formalism for fields  $B < B_0$  which is density dependent and typically lies between 0.3 and 1 T. Only at much higher fields does the single-particle SCBA become valid. The normalized conductivity  $\sigma^*(B)$  is density dependent in the crossover region in contrast to both the Drude and SCBA models. This, as well as the very fact that the Drude model holds for  $\mu B \gg 1$ , is a key indicator of many-electron effects. This Letter presents the first experimental demonstration of this density dependence in the magnetoconductivity of a nondegenerate 2DES. Previous measurements in a magnetic field [3,8–12] will be discussed below.

The conductivity of the 2DES on liquid helium was measured using the Corbino geometry with circular electrodes beneath the surface of the helium [3,13]. To obtain the best possible electrode structure, we used opti-

cal lithography and the precision device fabrication techniques of the Southampton University Microelectronics Centre [14]. The geometry of the Corbino disk, with six coplanar electrodes on polished fused quartz, is shown in Fig. 1. A central (or drive) electrode  $A$  was surrounded by a ring electrode  $E$  which also separated the annular receiving electrode  $B$  into three segments  $B1$ ,  $B2$ , and  $B3$ . Around these was a planar guard electrode  $G$ . Two metallic gold layers were deposited, insulated by an intervening  $\text{SiO}_2$  layer. The electrodes were all in the upper metal layer. Electrical contact to the inner electrodes was made along strips in the lower metal layer which ran under the guard  $G$  and electrode  $E$ . These made contact to the upper metal electrodes through paths etched in the  $\text{SiO}_2$  dielectric layer. Finally,  $25 \mu\text{m}$  gold wires were bonded to pads on the outside of the  $5 \text{ mm} \times 5 \text{ mm}$  quartz chip.

The Corbino disk was placed in an experimental cell filled with ultrapure  $^4\text{He}$  [15]. Electrons were produced by glow discharge and held in place by dc potentials on electrodes  $A$ ,  $B$ , and  $E$  (dc ground), the guard electrode  $G(-ve)$  and a top plate  $(-ve)$   $1.6 \text{ mm}$  above the helium surface. The diameter of the electron sheet was  $4 \text{ mm}$ . An ac voltage  $V_0$  (typically  $10 \text{ mV}$ ) at a frequency  $f(= \omega/2\pi)$  between  $2$  and  $70 \text{ kHz}$  was applied to electrode  $A$  and the ac current,  $I$ , to the electrodes  $B$  was measured. Electrode  $E$  was kept at ac ground. The gap between neighboring electrodes was only  $10 \mu\text{m}$  and so we were able to set the depth  $d$  of the helium above the electrodes to be  $60 \mu\text{m}$  or less (an order of magnitude lower than any previous Corbino experiment) while maintaining a uniform electron density. This gave many significant advantages. The helium surface was leveled to better than  $1 \mu\text{m}$  by balancing the ac currents between the central electrode and the three segments of electrode  $B$ , as the cryostat was tilted. The fractional change in these three signals on tilting also enabled the depth of the helium to be determined. For  $d = 60 \mu\text{m}$  the electron density was very uniform and the width of the edge layer was only  $3\%$  of the radius. Finally the electron density (crucial for these experiments) was accurately determined

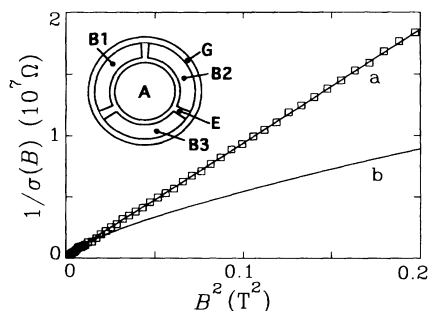


FIG. 1.  $1/\sigma(B)$  vs  $B^2$  for  $n = 1.49 \times 10^{12} \text{ m}^{-2}$  ( $\square$ ) at  $T = 1.3 \text{ K}$  for  $B < 0.5 \text{ T}$ . The lines show the Drude model (line  $a$ ) and the single-particle theory (line  $b$ ). [Inset: the Corbino electrode geometry.]

by increasing a  $-ve$  dc bias voltage on electrode  $E$  until the ac current between electrodes  $A$  and  $B$  cut off sharply. The density  $n$  was calculated from this cutoff voltage using a simple capacitance formula (allowing for the displaced electrons).

For a perfectly conducting electron sheet the phase of the capacitively coupled current  $I$  is  $\pi/2$  with respect to  $V_0$ . The phase shift  $\phi(B)$  away from  $\pi/2$  was measured as a function of  $B \leq 8 \text{ T}$  for a range of electron densities, for temperatures  $0.9 \leq T \leq 1.3 \text{ K}$ . The data cover a wide range of  $\mu B \leq 300$  and extend into the extreme quantum limit with  $\hbar\omega_c/kT \leq 10$ . For small phase shifts,  $\phi \leq 0.3 \text{ rad}$ , the conductivity is given by

$$\frac{1}{\sigma_{xx}(B)} = \frac{Ad}{\epsilon\epsilon_0\omega} \phi(B), \quad (2)$$

where  $A$  is a constant. For larger phase shifts the current amplitude and phase followed the theoretical response function for the 2D transmission line formed by the electrons and the underlying electrodes [13]. The high degree of circular symmetry in these precision electrodes meant that edge magnetoplasmons (EMP) [16] were not generated.

Figure 1 shows the measured conductivity for  $n = 1.49 \times 10^{12} \text{ m}^{-2}$  at  $1.3 \text{ K}$  in the low field range,  $B < 0.5 \text{ T}$ , plotted as  $1/\sigma$  versus  $B^2$ . All the low-field data followed the Drude result, Eq. (1), which enabled the mobility to be determined as  $23, 45, 100,$  and  $200 \text{ m}^2/\text{Vs}$  at  $1.30, 1.15, 1.00,$  and  $0.90 \text{ K}$ , close to previous measurements and the zero-field theoretical values [2,3]. The expected phase shifts at  $B = 0$  were well below the experimental resolution at these frequencies. Iye [3] used this method, and Eq. (1), in his pioneering measurements of  $\mu(T)$  from  $0.5$  to  $2 \text{ K}$ . His measurements were all at low field and he did not report any density dependence. More recently, Kovdya *et al.* [12] also reported  $1/\sigma(B) \propto B^2$  and a weak density dependence of  $\sigma^*(B)$  above  $1.5 \text{ K}$  in low fields. At  $1.3 \text{ K}$ , Fig. 1,  $\mu B = 1$  at  $0.04 \text{ T}$  ( $0.002 \text{ T}^2$  on the  $B^2$  axis plotted). Hence  $\mu B \gg 1$  for all the data presented here. In this region, the single-particle SCBA theory [8,10] predicts  $1/\sigma_s \propto (\mu B)^{3/2}$  as shown in Fig. 1. Both the field dependence and magnitude disagree with the experimental data. No scaling of  $\mu$  or other parameters can produce a satisfactory fit. The strong conclusion from this and previous work is that the Drude model holds, even for  $\mu B \gg 1$ , in low fields.

In slightly higher fields the situation changes dramatically as shown in Fig. 2(a) where  $\sigma(0)/\sigma(B)$  is plotted versus  $B^2$  for fields up to  $2 \text{ T}$  at  $1.3 \text{ K}$  for  $n = 2.78, 1.49, 1.04,$  and  $0.67 \times 10^{12} \text{ m}^{-2}$ . The lines  $a$  and  $b$  show the Drude and SCBA results, which are independent of density on this plot. The experimental results are clear. The data initially follow the Drude model but deviate above some field which increases with the electron density. This density dependence indicates that many electron effects are important in this field range.

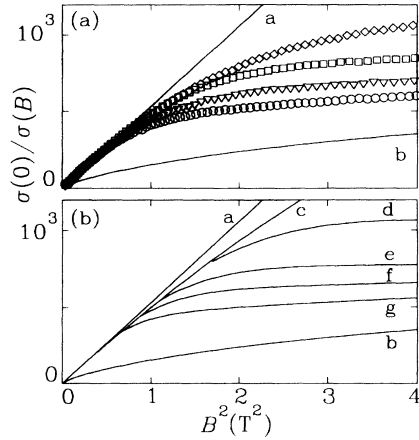


FIG. 2. (a)  $\sigma(0)/\sigma(B)$  vs  $B^2$  for  $n = 2.78$  ( $\diamond$ ),  $1.49$  ( $\square$ ),  $1.04$  ( $\nabla$ ), and  $0.67$  ( $\circ$ )  $\times 10^{12} \text{ m}^{-2}$  at  $T = 1.3 \text{ K}$  for  $B \leq 2 \text{ T}$ ; (b) the many electron theory  $1/\sigma_r^*$  for the same densities (lines  $d$ - $g$ ). The other lines show the Drude model ( $a$ ), the single-electron theory  $1/\sigma_s^*$  ( $b$ ), and the quantum-corrected Drude model ( $c$ ).

We now compare these measurements with the many-electron theory given by Dykman *et al.* [6]. The basic ideas can be simply understood in terms of cyclotron orbit diffusion [17]. The diffusion rate for elastic scattering depends on the spread of energies of neighboring orbits (the larger the spread, the smaller the diffusion rate). In the single-particle SCBA this is the Landau level collision width  $\hbar/\tau$ . But for a fluctuating many-electron field of magnitude  $\mathcal{E} \approx 0.84(kTn^{3/2}/\epsilon_0)^{1/2}$  [4-6], there are two other characteristic energy spreads: quantum uncertainty of the kinetic energy  $e\mathcal{E}\lambda_T$  ( $\lambda_T$  is the thermal wavelength) and the energy variation across a cyclotron orbit, radius  $R$ ,  $\Delta E \approx e\mathcal{E}R$ . For  $e\mathcal{E}\lambda_T > \hbar\omega_c$  the diffusion is essentially the same as in the Drude formalism; only for  $e\mathcal{E}\lambda_T < \hbar\omega_c$  and  $\Delta E < \hbar\omega_c$ , do the Landau levels influence the magnetoconductivity. This condition is equivalent to  $B > B_0 = 1.66 \times 10^{-5} n^{3/8} T^{1/2}$ , where  $B_0$  is the onset field for magnetoresistance. At high densities, such that  $B < B_0$ ,  $\sigma^*(B)$  will deviate from the classical Drude model, Eq. (1), because of quantum corrections to the diffusion length [in the quantum limit this becomes the magnetic length  $l = (\hbar/eB)^{1/2}$ ] and electron velocity. Then  $\rho^*(B)$  and  $\sigma^*(B)$  depend on  $\hbar\omega_c/kT$  but are independent of  $n$ . The first term in the expansion of  $\rho^*(B)$  is then [6]

$$\rho_m^* = 1 + \frac{5}{96} \left( \frac{\hbar\omega_c}{kT} \right)^2 \quad (3)$$

and  $\sigma_{xx} = \rho_{xx}/(\rho_{xx}^2 + \rho_{xy}^2)$  where  $\rho_{xy} = B/ne$  [10]. This high-density limit, or quantum-corrected Drude model, in which the scattering is field independent but allowance is made for the quantum cyclotron radius, is shown in Fig. 2 (line  $c$ ) and at  $1.3 \text{ K}$  deviates from the classical Drude model above  $1 \text{ T}$ .

At lower densities, the many-electron theory gives a density dependent factor for the normalized magnetoresis-

tivity which for  $\hbar\omega_c/kT < 1$  (but  $\mu B \gg 1$  as throughout) is given by [6]

$$\rho_m^* = \sum_{s=-\infty}^{\infty} [1 + 4\pi^2 s^2 (B_0/B)^4]^{-3/2}. \quad (4)$$

The density dependence of  $\sigma^*(B)$  comes from  $B_0$  which is  $0.88, 0.69, 0.61,$  and  $0.51 \text{ T}$  for the densities plotted in Fig. 2(a). In the limit of very low density the magnetotransport will be given by the noninteracting SCBA result of  $\rho_s$  and  $\sigma_s$  (line  $b$  in the figures). The combined theoretical resistivity,  $\rho_t$ , allowing for both many-electron effects and collisions can be estimated from

$$\frac{1}{\rho_t} = \frac{1}{\rho_m} + \frac{\rho_t}{\rho_s^2} \quad (5)$$

which was derived from the Einstein diffusion equation, allowing for the self-consistent nature of the SCBA, in which the scattering rate is proportional to  $\hbar\omega_c/\Gamma$ , where  $\Gamma$  is the energy uncertainty of each Landau level [18]. Note that this is not the combination of two different scattering mechanisms but the effect of the density of states on the scattering by vapor atoms. The normalized magnetoconductivity  $\sigma_r^*$  is plotted in Fig. 2(b) (lines  $d$  to  $g$ ) for the same densities as in Fig. 2(a) and shows very satisfactory agreement with the data, especially as there are no adjustable parameters in the calculations. The density dependence of  $1/\sigma^*(B)$  is clearly reproduced.

Measurements up to  $8 \text{ T}$  are shown in Fig. 3. In this range, the density dependence of  $1/\sigma^*(B)$  becomes less and the data approach the single-particle SCBA result as the field increases. At higher fields the energy spread  $\Delta E$  due to the many-electron fields decreases and becomes smaller than the collision width of the Landau levels. However, it can still be significant and  $\rho_m^*$  and  $\sigma_m^*$  have been calculated in the quantum limit,  $\hbar\omega_c/kT > 1$ , from [5,6]

$$\rho_m^* = 0.15(\omega_c/\omega_p)(\hbar\omega_c/kT)^{3/2}, \quad (6)$$

where  $\omega_p = (e^2 n^{3/2}/2\epsilon_0 m)^{1/2}$  is the characteristic plasma frequency of the 2DES. The theoretical magnetoconduc-

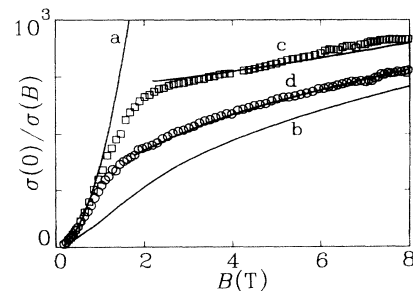


FIG. 3.  $\sigma(0)/\sigma(B)$  vs  $B$  for  $n = 2.34$  ( $\square$ ) and  $0.74$  ( $\circ$ )  $\times 10^{12} \text{ m}^{-2}$ ,  $T = 1.3 \text{ K}$  for  $B \leq 8 \text{ T}$ . The lines show the Drude model ( $a$ ), the single-electron theory  $1/\sigma_s^*$  ( $b$ ), and the many-electron conductivity  $1/\sigma_r^*$  ( $c$ ) and ( $d$ ).

tivity  $\sigma_i^*$  in this range is shown in Fig. 3 and again shows excellent agreement with the data. Only at higher fields, higher temperatures (low zero-field mobilities), and lower electron densities [9–11], does the single-electron SCBA theory alone give an adequate account of the magnetoconductivity in this system.

In conclusion, we have presented new measurements of the magnetoconductivity of a nondegenerate 2DES using high-precision Corbino electrodes. We have demonstrated, for the first time, the density dependence in the normalized conductivity  $\sigma^*(B)$  due to the influence of many-electron electric fields on the quantized Landau levels and the diffusion of cyclotron orbits. Calculations using the many electron theory of Dykman *et al.* [6] show excellent agreement with the data. It should be stressed that these many-electron effects arise from the long-range Coulomb interactions between electrons and not from the overlap of electron wave functions. These new results help in understanding the electronic transport in a nondegenerate 2D system where the Coulomb energy of the electron-electron interaction is larger than the thermal energy.

We would like to thank Mark Dykman, Rob van der Heijden, Peter Peters, and Peter Sommerfeld for many useful discussions. We thank the Engineering and Physical Science Research Council (U.K.) for a Research Grant and for a Studentship (for P.J.R.); A.K. Betts, F. Greenough, and J. Taylor for technical assistance; Donal Murphy, Andrew Jury, and the staff of the Southampton University Microelectronics Centre and the lithography unit of the Rutherford Appleton Laboratory.

- [1] For an introductory review see W.F. Vinen and A.J. Dahm, *Phys. Today* **40**, No. 2, 43 (1987).  
 [2] Yu. P. Monarkha, *Fiz. Nizk. Temp.* **2**, 1232 (1976) [*Sov. J. Low Temp. Phys.* **2**, 600 (1976)]. M. Saitoh, *J. Phys. Soc. Jpn.* **42**, 201 (1977); *Solid State Commun.* **52**, 63 (1984).  
 [3] Y. Iye, *J. Low Temp. Phys.* **40**, 441 (1980).  
 [4] M.I. Dykman and L. S. Khazan, *Zh. Eksp. Teor. Fiz.* **77**, 1488 (1979) [*Sov. Phys. JETP* **50**, 747 (1979)].  
 [5] M.I. Dykman, *Fiz. Nizk. Temp.* **6**, 560 (1980) [*Sov. J. Low Temp. Phys.* **6**, 268 (1980)]; *J. Phys. C* **15**, 7397 (1982).  
 [6] M.I. Dykman, M.J. Lea, P. Fozooni, and J. Frost, *Phys. Rev. Lett.* **70**, 3975 (1993).  
 [7] T. Ando and Y. Uemura, *J. Phys. Soc. Jpn.* **36**, 959

- (1974); T. Ando, Y. Matsumoto, and Y. Uemura, *J. Phys. Soc. Jpn.* **39**, 279 (1974); T. Ando, A.B. Fowler, and F. Stern, *Rev. Mod. Phys.* **54**, 437 (1982).  
 [8] R.W. van der Heijden, M.C.M. van de Sanden, J.H.G. Surewaard, A.Th.A.M. de Waele, H.M. Gijsman, and F.M. Peeters, *Europhys. Lett.* **6**, 75 (1988).  
 [9] J. Neuenschwander, P. Scheuzger, W. Joss, and P. Wyder, *Physica (Amsterdam)* **165 & 166B**, 845 (1990); P. Scheuzger, J. Neuenschwander, and P. Wyder, *Helv. Phys. Acta* **64**, 170 (1991); P. Scheuzger, J. Neuenschwander, W. Joss, and P. Wyder, *Helv. Phys. Acta* **65**, 325 (1992); *Physica (Amsterdam)* **194-196B**, 1231 (1994).  
 [10] Yu. P. Monarkha, *Fiz. Nizk. Temp.* **19**, 737 (1993) [*Sov. J. Low Temp. Phys.* **19**, 530 (1993)]. P.J.M. Peters, P. Scheuzger, M.J. Lea, Yu. P. Monarkha, P.K.H. Sommerfeld, and R.W. van der Heijden, *Phys. Rev. B* (to be published).  
 [11] P.W. Adams and M.A. Paalanen, *Phys. Rev.* **32**, 3805 (1988).  
 [12] Yu.Z. Kovdrya, V.A. Nikolayenko, O.I. Kirichek, S.S. Sokolov, and V.N. Grigor'ev, *J. Low Temp. Phys.* **91**, 371 (1993).  
 [13] R. Mehrotra and A. Dahm, *J. Low Temp. Phys.* **67**, 115 (1987); L. Wilen and R. Giannetta, *J. Low Temp. Phys.* **72**, 353 (1988). Yu. P. Monarkha and P.K.H. Sommerfeld (private communication).  
 [14] A. Blackburn *et al.* (to be published).  
 [15] Supplied by Professor P. V. E. McClintock, Department of Physics, University of Lancaster, United Kingdom. The  $^3\text{He}/^4\text{He}$  atomic ratio was less than  $10^{-13}$ .  
 [16] P.J.M. Peters, M.J. Lea, A.M.L. Janssen, A.O. Stone, W.P.N.M. Jacobs, P. Fozooni, and R.W. van der Heijden, *Phys. Rev. Lett.* **67**, 2199 (1991).  
 [17] M.J. Lea and M.I. Dykman, *Philos. Mag. B* **69**, 1059 (1994).  
 [18] The Einstein relation for  $\mu B \gg 1$ , gives  $\sigma \propto \rho_t = A/\tau_B$  in a field  $B$ . If the cyclotron orbits have a spread of energies  $\Gamma$  then the scattering rate is enhanced, due to the concentration of the density states (uniform in zero field) into Landau levels, by a factor  $\hbar\omega_c/\Gamma$ . If we write  $\Gamma = \hbar/\tau_B + \Gamma_m$  as the sum of collision broadening and many-electron effects then

$$\frac{1}{\tau_B} \approx \frac{1}{\tau_0} \frac{\hbar\omega_c}{\Gamma_m + \hbar/\tau_B} \quad \text{or} \quad \tau_B \approx \frac{\Gamma_m\tau_0}{\hbar\omega_c} + \frac{\tau_0}{\omega_c\tau_B}.$$

For  $\Gamma_m = 0$ , this gives the SCBA result,  $\rho_s = (A/\tau_0)\sqrt{\omega_c\tau_0}$  while for many-electron fields only,  $\rho_m = (A/\tau_0)(\hbar\omega_c/\Gamma_m)$ . Hence, in combination,  $1/\rho_t = 1/\rho_m + \rho_t/\rho_s^2$ .